

S. Kim¹, J. Xu², L. Moy¹, H. Rusinek¹, and D. K. Sodickson¹¹Center for Biomedical Imaging, Department of Radiology, New York University, New York, NY, United States, ²Siemens Medical Solutions USA Inc., New York, NY, United States

Introduction: Accurate quantification of water and fat components has important potential applications in characterizing tumors, fatty liver, breast and ischemic heart (1-4). Chemical shift-based multipoint water-fat separation methods, i.e. Dixon methods (1), have been widely used among the MRI methods to date. Two-point Dixon method is often a preferred choice (over three-point Dixon method) as shorter scan time reduces the motion artifacts which represent potential sources for processing failure (2). However, the fat and water images from the two-point Dixon method often exhibit intensity inhomogeneity partly due to the inhomogeneous RF coil sensitivity. The objective of this study was to develop a novel image processing method to correct the intensity inhomogeneity in two-point Dixon images without additional information.

Materials and Methods:

MRI data were acquired from a phantom containing an orange in canola oil and from two human subjects, using a whole body Siemens 3T Tim Trio system and a 7-element breast coil array. A 3D FLASH sequence was used with TR=8.53 ms, TE1=2.45 ms, TE2=6.125 ms, FA=12°, iPAT=2, and spatial resolution = 0.9 x 0.6 x 1.0 mm. The institutional review board approved this study, and written informed consent was obtained from all subjects before the scans.

The intensity correction algorithm was developed based on the relationship between two-point Dixon water (I_w) and fat (I_f) images. Both of them can have intensity inhomogeneity as demonstrated by the phantom images shown in Fig.1a and 1e. Fat and water fractions are defined as $F_f = I_f / (I_w + I_f)$ and $F_w = I_w / (I_w + I_f)$, respectively. As shown in Fig.1b and 1f, both fat and water fraction images have similar anatomical features as the fat and water images, but without appreciable intensity inhomogeneity. Assuming that the intensity inhomogeneity in the uncorrected images varies slowly across the image, the intensity correction map (I_c) was estimated as a combination of 2D discrete cosine bases (up to the 2nd order). The weighting factors of the bases for the combination were estimated to minimize the sum of $(F_f - I_f/I_c)^2$ and $(F_w - I_w/I_c)^2$ using Simplex method. The estimation of the correction map was performed only with the region above the maximum of the background noise. The examples of the estimated correction maps for the phantom are shown in Fig.1c and 1g. The corrected image was obtained by dividing the uncorrected image by the correction map (I_f/I_c or I_w/I_c). Finally, the mean intensity of the corrected image was adjusted to that of the uncorrected image. The corrected images shown in Fig.1d and 1h demonstrate successful application of this method with the phantom image.

Results and Discussion:

Fig.2 shows a representative example of the result from one subject. The red arrow in Fig.2a points to a region where the image intensity is unusually high whereas the yellow arrow indicates the area where the image intensity drops rapidly following the coil sensitivity drop out. This effect is less prominent in the water image (Fig.2e), but the signal drop out can be noticed in the similar location as in Fig.2a. The proposed method was successfully used to estimate the intensity correction maps shown in Fig.2c and 2g. The correction maps correspond well with the visual observation of the intensity inhomogeneity in Fig.2a and e. The corrected fat (Fig.2d) and water (Fig.2h) images show noticeable increase of the intensity homogeneity across the whole image plane. Substantial improvement can be noticed in the areas pointed by the arrows where severe inhomogeneity was noticed in the uncorrected images. This was consistently observed with the rest of the images. Fig.3 presents the effect of the correction in terms of change in the histogram. In both fat and water, the uncorrected images (black lines) have diffuse distributions of signal intensity. In contrast, the corrected images (red lines) have more narrow peaks, suggesting reduced variability in the signal intensity within fat and water compartments. This result suggests that our method can be used to improve the quantification of fat, especially in clinical imaging applications where a two-point Dixon method is preferred to minimize motion artifact.

Reference: 1. Dixon, W.T. (1984) Radiology 153:189-194. 2. Ma, J. (2008) JMRI 28: 543-558. 3. Kim, H. et al. (2008) MRM 59:521-527. 4. Bernard C.P. et al. (2008) JMRI 27:192-197.

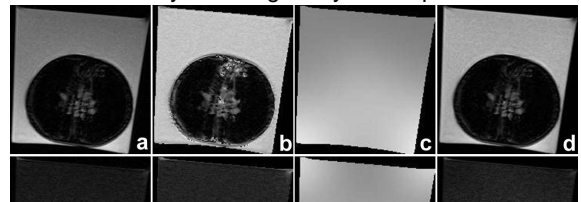


Figure 1. Phantom test. (a) fat, (b) fat fraction, (c) estimated correction map for fat image shown in (a), (d) corrected fat, (e) water, (f) water fraction, (g) estimated correction map for water image in (e), (h) corrected water image.

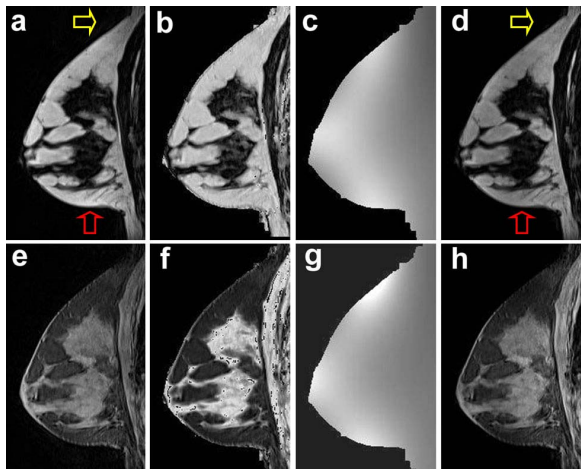


Figure 2. Result with healthy subject. (a) fat, (b) fat fraction, (c) estimated correction map for fat image shown in (a), (d) corrected fat, (e) water, (f) water fraction, (g) estimated correction map for water image in (e), (h) corrected water image.

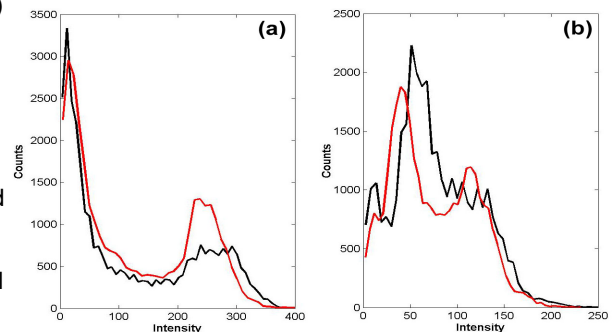


Figure 3. Comparison of histogram for fat(a) and water(b). Black lines are without correction. Red lines are after correction.